

PACS numbers: 42.55.Px; 85.60.Jb
DOI: 10.1070/QE2007v037n11ABEH013556

High-power multimode superluminescent diode emitting at 840 nm

E.V. Andreeva, D.V. Batrak, A.P. Bogatov, P.I. Lapin, V.V. Prokhorov, S.D. Yakubovich

Abstract. **Superluminescent diodes based on a single-layer quantum-well (GaAl)As heterostructure with the ridge active channel of width 25 μm are studied. At moderate levels of the injection current density and radiation load on the output facets the output cw power above 200 mW is obtained. The efficiency of coupling radiation into a standard multimode fibre is 75 %.**

Keywords: *superluminescent diode, multimode ridge waveguide.*

1. Introduction

Many specialised illumination systems (in microscopy, machine vision, etc.) require small radiation sources with a high brightness and a low coherence degree. At present high-brightness light-emitting diodes (HB LEDs) dominate in this field. However, HB LEDs can compete neither in the brightness of their radiation nor in the efficiency of coupling radiation into fibres with superluminescent diodes (SLDs). Almost all commercial SLDs have the single-mode active channel of width $W = 2 - 6$ μm. This provides a stable and smooth radiation pattern of SLD modules emitting into open space and also allows the fabrication of highly efficient SLD modules with single-mode fibre (SMF) pigtails to couple out radiation. The maximum cw output power of SLD modules of the first and second types does not exceed 50 and 20 – 30 mW, respectively. These limits in the near IR range between 780 and 1100 nm [SLDs based on (GaAl)As and (InGa)As heterostructures] are determined by degradation processes, and for the spectral range from 1250 to 1700 nm [SLDs based on (InGa)PAs heterostructures] – by thermal processes due to a greater stability of these SLDs with respect to degradation but their lower quantum efficiency.

The obvious solution in the development of high-power and reliable SLDs with moderate current and radiation loads in the active channel became the use of structures with a broad active waveguide ($W > 20$ μm). This approach is often used in high-power laser diodes (LDs). In most laser heterostructures using conventional methods of lateral optical confinement, such waveguides are multimode. Many practical applications require radiation sources with symmetric and smooth radiation patterns. This is an important problem in the optimisation of designs and operation regimes of high-power LDs. In the case of SLDs of the traditional design with the active channel directed at an angle to the crystal end-facets, additional difficulties can appear due to excitation of parasitic lasing in the direction perpendicular to these facets. At the dawn of the development of SLDs in the early 1970s, due to technical limitations only samples with broad active channels were studied [1 – 3] (paper [2] was performed in 1970 – 1971). In [4], requirements to the SLD parameters excluding excitation of the above-mentioned parasitic lasing were analysed apparently for the first time. These requirements impose certain restrictions on the relation between the width W and length L_a of the active channel in a SLD depending on its waveguide and amplification parameters and the inclination angle of its axis.

The aim of our paper was to develop a reliable SLD emitting above 100 mW of cw power in the spectral range between 830 and 850 nm, which could be coupled with a standard multimode fibre (MMF) with a core diameter of 50 μm. According to the latter requirement, the active channel width was chosen to be 25 μm. We calculated the mode composition and near- and far-field radiation intensity distributions depending on the pump level for the SLD with the ridge active waveguide of this width based on the traditional (GaAl)As heterostructure with the quantum-well active layer and separate confinement. The results of calculation well agree with the output parameters of experimental samples. The results of preliminary resource tests of the prototypes of high-power multimode SLD modules are presented.

2. Experimental samples

Figure 1 shows the structure of experimental SLD samples. We fabricated and studied samples of two types with active channel axes directed at angles $\alpha_1 = 12.5^\circ$ and $\alpha_2 = 7.0^\circ$ with respect to the normal to the crystal end-facets covered with AR coatings. The maximum length of the active channel was 1400 and 1600 μm for samples with inclination angles α_1 and α_2, respectively. Metal contacts and a ZnSe dielectric mask with a strip window providing the local

E.V. Andreeva, P.I. Lapin, V.V. Prokhorov Superlumdiodes Limited Liability Company, P.O. Box 70, 117454 Moscow, Russia;
D.V. Batrak, A.P. Bogatov P.N. Lebedev Physics Institute, Russian Academy of Sciences, Leninsky prosp. 53, 119991 Moscow, Russia
S.D. Yakubovich Moscow State Institute of Radio Engineering, Electronics and Automatics (Technical University), prosp. Vernadskogo 78, 117454 Moscow, Russia; e-mail: yakubovich@superlumdiodes.com

Received 5 March 2007; revision received 2 April 2007
Kvantovaya Elektronika **37** (11) 996 – 1000 (2007)
Translated by M.N. Sapozhnikov

injection of charge carriers into the active channel are not shown in Fig. 1. The 14.5-nm-thick active layer was located in the waveguide layer between two undoped 0.12-μm-thick $Al_{0.4}Ga_{0.6}As$ layers. The lateral optical confinement was provided by a mesa structure of width $W = 25$ μm produced by ion etching. The waveguide properties of this structure are determined by its geometry, in particular, by the thickness δ of the 'incompletely etched' layer up to the upper boundary of the waveguide layer (the residual thickness of the cladding layer) and the relation of the refractive indices of the waveguide and emitter layers. The thickness δ of the samples studied was 0.20–0.25 μm. Due to a large enough width of the waveguide, several transverse modes with different field distributions in the p–n junction plane can propagate in it. By determining contributions of each of these modes to the output superluminescence emission, one should take into account, along with the properties of the 'cold' waveguide, the antiwaveguide effect related to the injection of carriers and the influence of the temperature distribution in the crystal on the waveguide properties of the active channel.

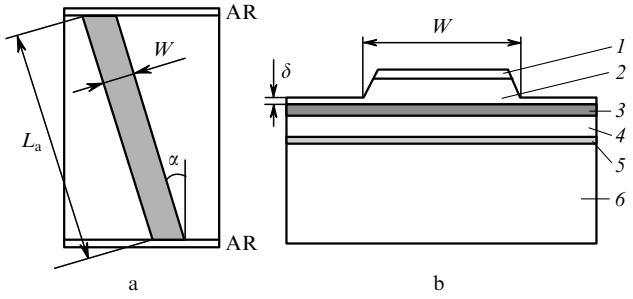

Figure 1. Configuration of the active channel of an SLD (a) and its cross section (b): (*1*) contact p^+-GaAs layer; (*2*) $Al_{0.6}Ga_{0.4}As$ p-emitter; (*3*) 0.25-μm-thick $Al_{0.4}Ga_{0.6}As$ waveguide layer with the active quantum-well layer; (*4*) $Al_{0.6}Ga_{0.4}As$ n-emitter; (*5*) buffer layer; (*6*) n^+-GaAs substrate.

3. Calculation of the spatial parameters of radiation of a transversely multimode SLD

The propagation of radiation in the SLD was calculated in the approximation of the effective refractive index n_{eff}, i.e. in two dimensions (in the heterojunction plane yz). The spatial profile of n_{eff} was determined by the contribution Δn_{wg} of the built-in waveguide, the temperature contribution Δn_T, and the contribution depending on the carrier concentration Δn_N in the active medium, whose complex part was determined in turn by the gain in the active medium. It was assumed that the z axis was directed along the active channel, i.e. in the radiation propagation direction. It was also assumed that the properties of the medium are independent of the coordinate z [we neglect the inhomogeneous (along the longitudinal coordinate) burning of carriers]. Thus,

$$n_{\text{eff}}(y) = n_0 + \Delta n_{\text{wg}}(y) + \Delta n_T(y) + \Delta n_N(N(y)),$$
$$\text{Im}\, n_{\text{eff}}(y) = \text{Im}\, \Delta n_N(y) = -\frac{\lambda_0}{4\pi} g(N(y)), \quad (1)$$

where λ_0 is the radiation wavelength in vacuum and $g(N)$ is the effective (mode) gain.

In the case under study, the field in the SLD can be expanded in the transverse modes of the system, i.e. the y component of the electric field (assuming that radiation has the TE polarisation) in the single-frequency approximation can be written in the form

$$E(y,z) = \exp(-\text{i}\omega t)$$
$$\times \sum_m C_m(z) U_m(y) \exp(\text{i}\beta_m z) + \text{c.c.}, \quad (2)$$

where $C_m(z)$ are the amplitudes of transverse modes, and the distributions of fields of the modes $U_m(y)$ and their propagation constants β_m are determined by the waveguide, i.e. by the dependence $n_{\text{eff}}(y)$. Strictly speaking, the field should be expanded in a complete set of transverse modes, which includes a discrete set of guided modes and a continuum of radiation modes. However, we neglect the latter because amplification takes place for guided modes localised in the pumped region. Expression (2) describes radiation propagating in the positive direction of the z axis (for counterpropagating radiation, a similar expression is valid).

By substituting expression (2) for the field into the wave equation, which contains random Langevin sources simulating spontaneous radiation, we can obtain the equation for $C_m(z)$ and calculate expressions $\langle C_m(z) C^*_{m'}(z)\rangle$ determining the intensities of individual modes (for $m = m'$) and correlations between modes (for $m \neq m'$) [5]. By knowing $\langle C_m(z) C^*_{m'}(z)\rangle$, we can calculate any quadratic function of field (2), including the near- and far-field radiation intensity distributions.

The carrier concentrations $N(y)$ were determined from the balance equation

$$\frac{N(y)}{\tau} + \kappa g(N(y)) S(y) + D \frac{\text{d}^2 N(y)}{\text{d}y^2} = J(y), \quad (3)$$

where the first term in the left-hand side of the equation describes the spontaneous recombination of carriers with the lifetime τ, the second term describes stimulated recombination with the rate proportional to the field intensity $S(y)$, the third term describes the diffusion of carriers (D is the diffusion coefficient), and the right-hand side of the equation describes the pump current.

This model allows us to calculate for the specified pump current the intensities of transverse modes inside the SLD and on the output mirror as well as the distribution of the carrier concentration self-consistently, i.e. taking into account the inhomogeneous (in the transverse direction along the y axis) burning of carriers. Numerical calculations are performed by using the following iteration procedure. The profile of the effective refractive index $n_{\text{eff}}(y)$ is calculated for an arbitrary initial distribution of the carrier concentration $N(y)$, then, by using the method described in [6], the propagation constants and distributions of the fields of coupled modes of such a waveguide are found. Then, the radiation intensity $S(y)$ is calculated and the left-hand side of Eqn (3) for carriers is calculated. Based on the residual, the distribution of carrier concentration $N(y)$ in this equation is modified and the procedure is repeated. The process is continued until the required accuracy is achieved.

Below, the results of calculation are presented for the SLD with $L_a = 1400$ μm, the width of the stripe pump region $W = 25$ μm, and the inclination angle of the active channel to the diode axis $\alpha = 12.5^\circ$. We used in calculations the typical parameters of semiconductor heterostructures (dependences of the gain and refractive index on the carrier concentration). Two variants of the SLD design with the residual thickness $\delta = 0.3$ or 0.2 μm of the cladding layer outside the stripe pump region were calculated (in the second case, the waveguide properties are stronger than in the first one). Calculations were performed taking into account or neglecting the induced temperature waveguide.

One can see from Fig. 2 that the width of the far-field intensity distribution increases with increasing pump current. This is explained by the increase in the relative intensity of transverse modes with greater indices (having a larger divergence). Taking the temperature waveguide into account, this effect leads, in particular, to the formation of the radiation pattern with a dip at the centre due to a decrease in the relative intensity of the zero transverse mode.

The spatial distributions of the output radiation of the SLD recorded with an LD8900/IR goniometer illustrate the dependence of the far-field pattern on the injection current (Fig. 3). Figure 4 presents the dependences of the width of the radiation pattern on the injection current calculated for

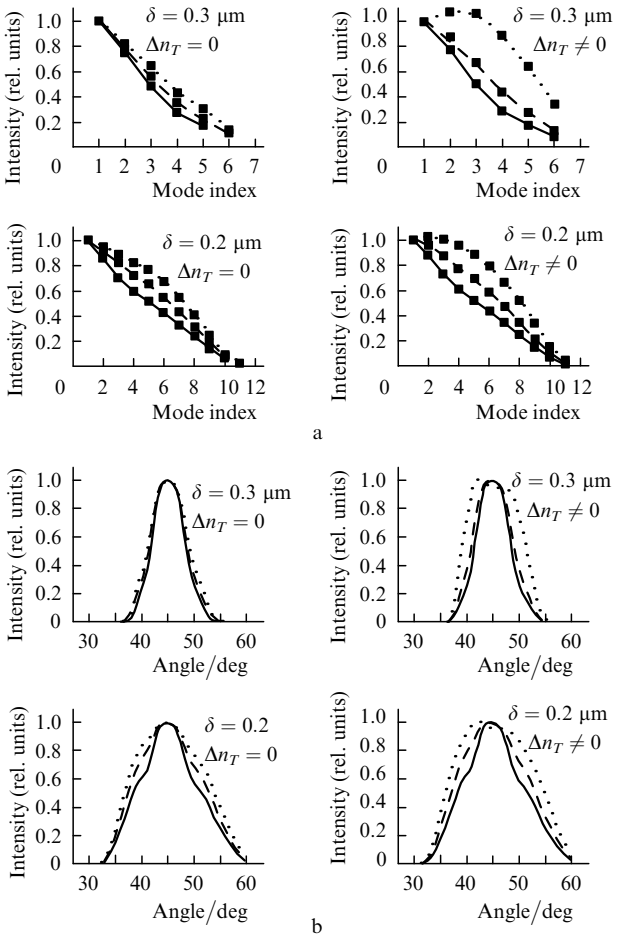

Figure 2. Relative intensities of transverse modes (a) and radiation patterns in the p–n junction plane (angles are counted off from the normal to the output face of the diode) (b) taking into account and neglecting a temperature waveguide for injection currents 300 (solid curves), 500 (dashed curves), and 1000 mA (dotted curves).

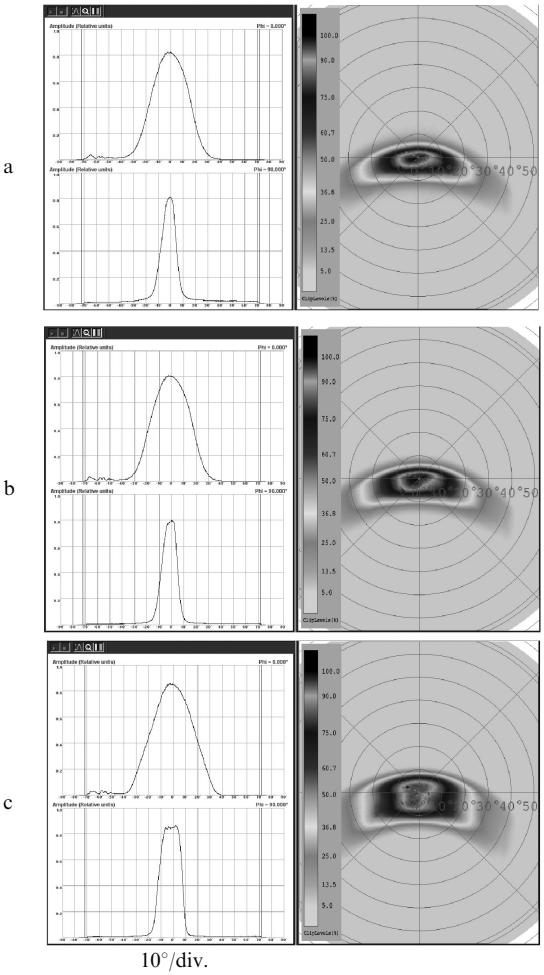

Figure 3. Angular far-field radiation intensity distributions in the plane perpendicular to the p–n junction (upper curves) and in the p–n junction plane (lower curves) (in the left), and cross sections of output beams (in the right). The injection currents are 300 (a), 500 (b), and 1000 mA (c).

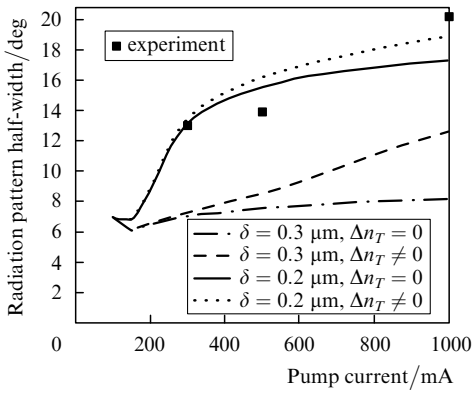

Figure 4. Dependences of the radiation divergence in the p–n junction plane on the injection current.

two values of the parameter δ. The curves corresponding to $\delta = 0.2$ μm well describe the experimental results.

4. Power, spectral and resource parameters

The aim of our paper was to develop high-power SLDs. Therefore, we did not fabricate samples with the active

channel length $L_a < 1200$ μm in which parasitic lasing can be excited. The power parameters of SLDs of both types (with different α) with the same active channel length were virtually identical. Figure 5 shows the typical light–current characteristic in the continuous injection regime for the SLD with $L_a = 1400$ μm. The total external efficiency in the superluminescence regime upon coupling out radiation to open space was about 0.7 W A^{-1}, which is only slightly less than that for the best laser diodes based on similar heterostructures. To couple radiation into standard MMFs with the 50-μm core diameter, cylindrical microlenses skewed at the corresponding angles were fabricated at the ends of fibres. The coupling efficiency amounted to 75 %.

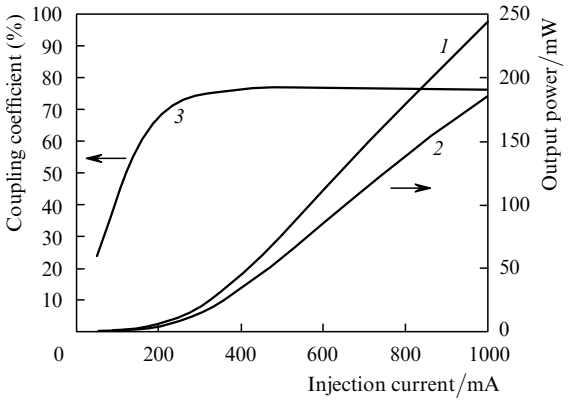

Figure 5. Typical light–current characteristics upon coupling out radiation to open space (*1*) and through a MMF (*2*), and the coupling coefficient (*3*).

The evolution of the output emission spectrum with increasing injection current is typical for SLDs based on a single-layer quantum-well heterostructure [7]. At high pump currents, quantum transitions from the first excited state dominate (Fig. 6). The short-wavelength spectral band has the half-width about 15 nm, which corresponds to the radiation coherence length about 50 μm. The depth of the residual spectral modulation produced by Fabry–Perot modes does not exceed 1 %. When radiation was coupled out of SLDs through a straight or slightly bent MMF, weakly pronounced speckles were observed in the far field,

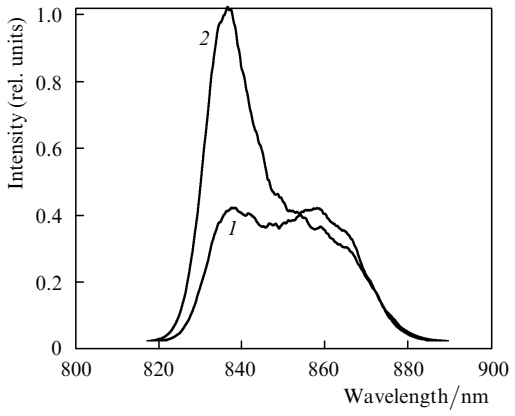

Figure 6. Emission spectra for injection currents 450 (*1*) and 750 mA (*2*).

their contrast being considerably lower than that observed for laser radiation coupled out under similar conditions. After winding the MMF on a coil of radius 4–6 cm, due to the coupling of fibre modes the output radiation pattern acquires the axially symmetric shape with a smooth bell intensity distribution and divergence corresponding to the numerical aperture of the MMF.

SLDs of the second type with $L_a = 1600$ μm were used to assemble light-emitting modules in Butterfly housings with MMF pigtails. Highly efficient Peltier coolers provided the operation of modules in the temperature range between −55 and +60°C at the SLD operation current up to 1.0 A and the SLD thermal stabilisation at 25 °C. A batch of these modules was preliminarily tested at a current of 750 mA, corresponding to the 110–120-mW output power through a MMF. Figure 7 presents the results of these tests. The estimated lifetime (during which the output power decreases by 50 %) was more than 5000 h, which is acceptable for many practical applications.

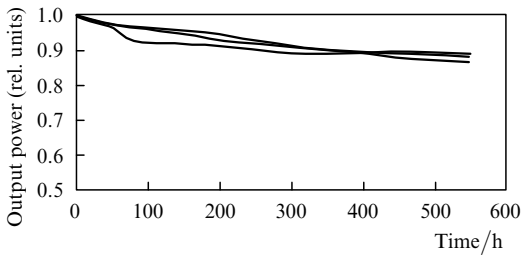

Figure 7. Results of resource tests of a batch of prototypes of multimode SLD modules for the injection current 750 mA.

It is well known that SLD modules with SMF pigtails are very sensitive to optical feedback [8]. First of all, this concerns high-power SLD modules, where feedback already at the −20-dB level can drastically change the output parameters and even cause the degradation of an SLD, which necessitates the use of expensive optical isolators. A useful feature of the developed SLD modules is their weak sensitivity to feedback, which is explained by a considerable difference in the structure of modes in a planar multimode waveguide, such as the active channel of a SLD, and in a MMF. Figure 8 presents the dependences of the output power coupled out of the MMF and the current of a photodiode built in the module (which is proportional to the output power emitted through the rear facet of the SLD) on the injection current for modules with the output end-facet of the MMF angled at 7° with respect to the normal to its axis, as is usually done in 'single-mode' SLD modules (FC/APC connector), and with the output end-facet of the MMF perpendicular to its axis. In the first case, the optical feedback is absent, while in the second case, it amounts to 4 % (−14 dB). One can see that the relative change in the forward and backward light fluxes in the presence of feedback does not exceed 10 % and cannot noticeably accelerate degradation.

5. Conclusions

At present more than one hundred types of SLD modules based on various heterostructures are being manufactured in series. The emission spectra of 'high-power' modules (above 10 mW of output power coupled out through a

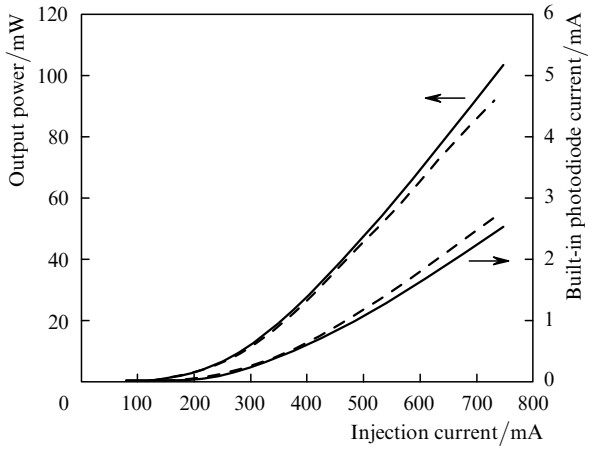

Figure 8. Dependences of the output power and current of a photodiode monitor on the injection current of a SLD for modules with the skewed end-face of the output MMF (solid curves) and with the normal end-face (dashed curves).

SMF) cover virtually the entire IR range from 780 to 1600 nm. It is obvious that, by using the same heterostructures and the SLD design, similar modules with MMF pigtails emitting such and higher output powers in this spectral range can be manufactured. The question of the relation between the maximum output power and reliability in each case requires a separate study.

Acknowledgements. The authors thank A.T. Semenov for initiating this work and P.A. Lobintsov for his help at its initial stage.

References

1. Kurbatov L.N., Shakhidzhanov S.S., Bystrova L.V., Karpukhin V.V., Kolonenkova S.I. *Fiz. Tekh. Poluprovodn.*, **4**, 1739 (1971).
2. Stupnikov V.A., Yakubovich S.D. *Elektron. Tekh., Ser. 11*, **5**, 62 (1978).
3. Lee T.P., Burrus C.A. Jr., Miller B.I. *IEEE J. Quantum Electron.*, **9**, 820 (2003).
4. Alphonse G.A., Gilbert D.B., Harvey M.G., Ettenberg M. *IEEE J. Quantum Electron.*, **24**, 2454 (1988).
5. Haus H.A., Kawakami S. *IEEE J. Quantum Electron.*, **21**, 63 (1985).
6. Stratonnikov A.A., Bogatov A.P., Drakin A.E., Kamenets F.F. *J. Opt. A: Pure Appl. Opt.*, **4**, 535 (2002).
7. Batovrin V.K., Garmash I.A., Gelikonov V.M., Gelikonov G.V., Lyubarskii A.V., Plyavenek A.G., Safin S.A., Semenov A.T., Shidlovskii V.R., Shramenko M.V., Yakubovich S.D. *Kvantovaya Elektron.*, **23**, 113 (1996) [*Quantum Electron.*, **26**, 109 (1996)].
8. Andreeva E.V., Shramenko M.V., Yakubovich S.D. *Kvantovaya Elektron.*, **37**, 443 (2007) [*Quantum Electron.*, **37**, 443 (2007)].